PROGRESS ON MUON IONIZATION COOLING DEMONSTRATION WITH MICE

NAPAC2019
Lansing, MI, USA

Author: Christopher Hunt, CERN
Presenter: Pavel Snopok, Illinois Institute of Technology
on behalf of the MICE Collaboration

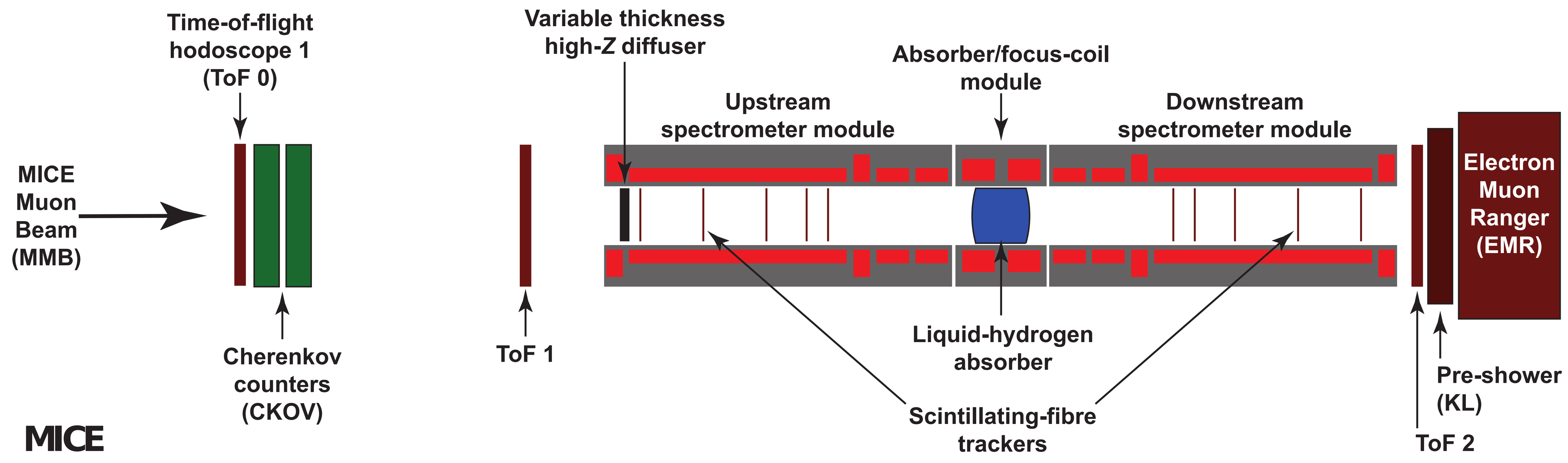

Figure 1: Schematic layout of the MICE cooling channel. Magnet coils are shown in red, the absorber in blue and the various detetectors are individually marked.

INTRODUCTION

The MICE experiment consists of an upstream beamline to capture pions emitted from the titanium target, and focus the produced muons into a cooling channel. The cooling channel (Figure 1) consists of 12 individually powered solenoid magnets, symmetrically placed up- and downstream of an absorber chamber which could be configured depending on the beam momentum and required beta-function. Upstream and downstream particle ID (PID) detectors are used to improve the reconstruction algorithms and reject pion and electron contamination within the beam. A range of absorbers were used during data taking including an empty drift space (no absorber), a 65 mm-thick lithium hydride disk (LiH), and a 22-l liquid hydrogen vessel (LH2).

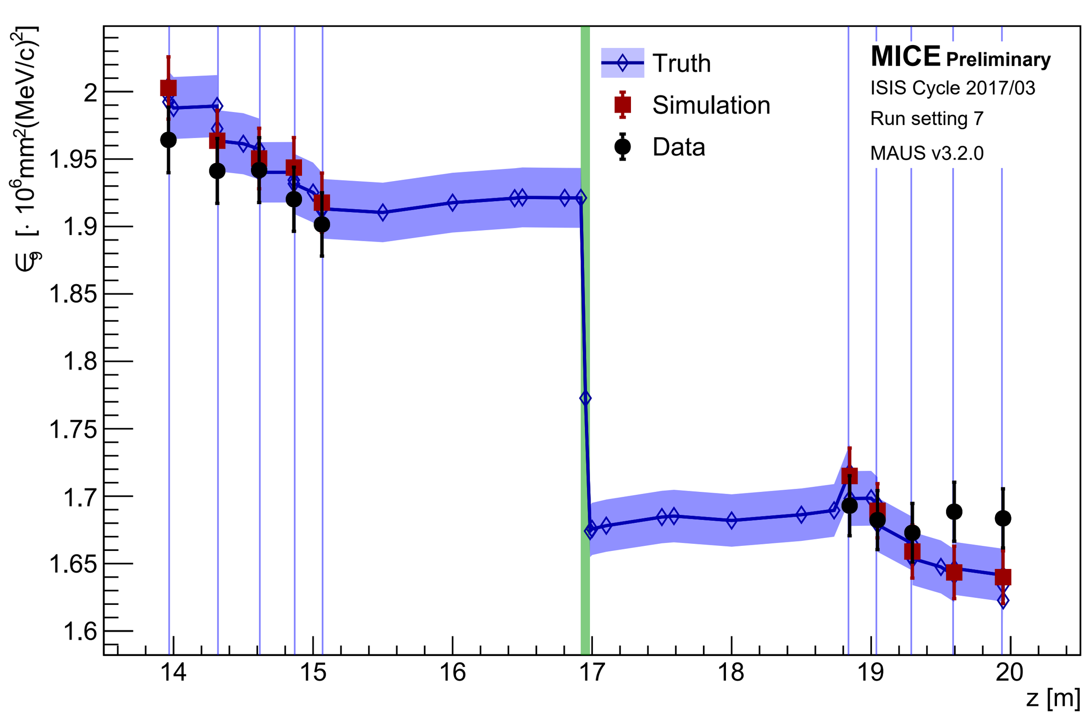

Figure 2: Evolution of the fractional emittance (9%) along the length of the cooling channel. 9% is the fraction of the beam particles contained in the RMS ellipse in 4D representing the core of the beam. Absorber material: LiH.

RECONSTRUCTION

The muon beam emittance was calculated by constructing the covariance matrix, Σ, using the covariances, σ_{ab}, of the position and momentum components of the individual muon tracks:

$$\Sigma = \begin{pmatrix} \sigma_{xx} & \sigma_{xp_x} & \sigma_{xy} & \sigma_{xp_y} \\ \sigma_{p_x x} & \sigma_{p_x p_x} & \sigma_{p_x y} & \sigma_{p_x p_y} \\ \sigma_{yx} & \sigma_{yp_x} & \sigma_{yy} & \sigma_{yp_y} \\ \sigma_{p_y x} & \sigma_{p_y p_x} & \sigma_{p_y y} & \sigma_{p_y p_y} \end{pmatrix}.$$

The 4-dimensional normalised transverse emittance, ϵ_{4D}, of the beam can then be calculated using the determinant of the covariance matrix and the muon mass, m_μ:

$$\epsilon_{4\mathrm{D}} = \frac{1}{m_\mu}\sqrt[4]{|\Sigma|}.$$

The single particle amplitude, $A_\perp$, at a point $v = (x, p_x, y, p_y)$ in phase-space can be defined as the square of the distance between v and the centre of the distribution in the phase-space normalised to the covariance matrix, weighted by the distribution's emittance. It estimates the emittance of a beam, which is characterised by an ellipse which passes through that point. It is calculated as

$$A_\perp = \epsilon_{4\mathrm{D}}\ (v - \bar{v})^{\mathrm{T}}\Sigma^{-1}(v - \bar{v}).$$

Events were selected with a time-of-flight consistent with a muon of momentum 140+/-5 MeV that did not cross any hard apertures that could cause scraping. The reconstructed upstream tracks were required to have good chi-square per degree of freedom values and be fully contained within the tracking volume. If a corresponding downstream track was also found it was subjected to the same goodness of fit criteria.

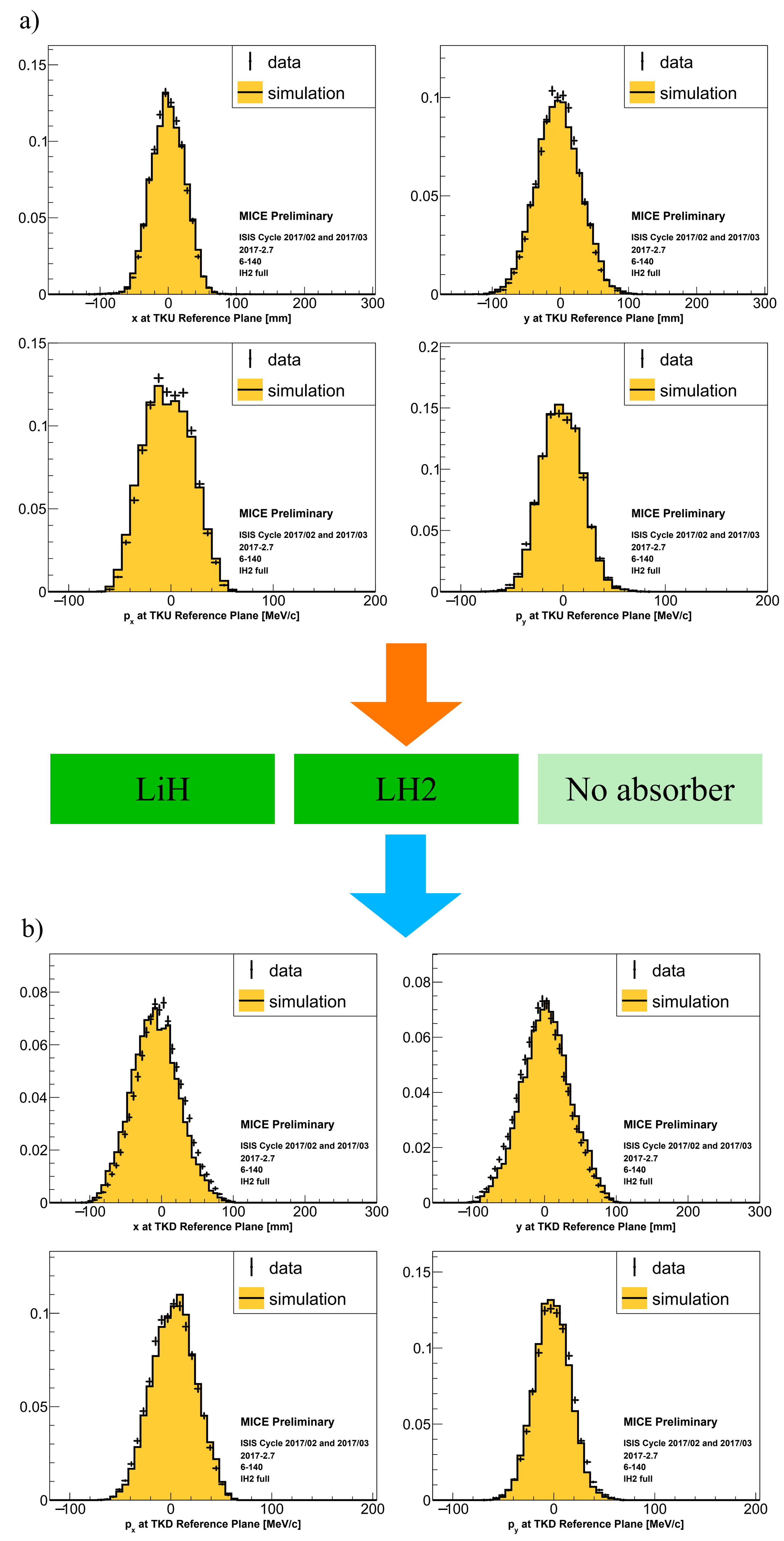

Figure 3: Distributions of the upstream (a) and downstream (b) position (top) and momentum (bottom) parameters in x (left) and y (right) for the LH2 data. All show good agreement between data and simulation.

EMITTANCE EVOLUTION

The distribution of amplitudes for the up- and downstream samples were integrated from zero, bin-by-bin to produce the cumulative distributions. The ratio of the cumulative distributions (R_{Amp}) is indicative of particle migration. As seen in Figure 4, the *No absorber* case demonstrates the effects of scraping, as muons at medium/high amplitudes migrate outwards and are lost.

The *LH2* and *LiH* cases demonstrate a clear increase in the particle density in the core of the beam, which is a signal of ionization cooling, a direct consequence of the presence of an absorber material in the cooling channel.

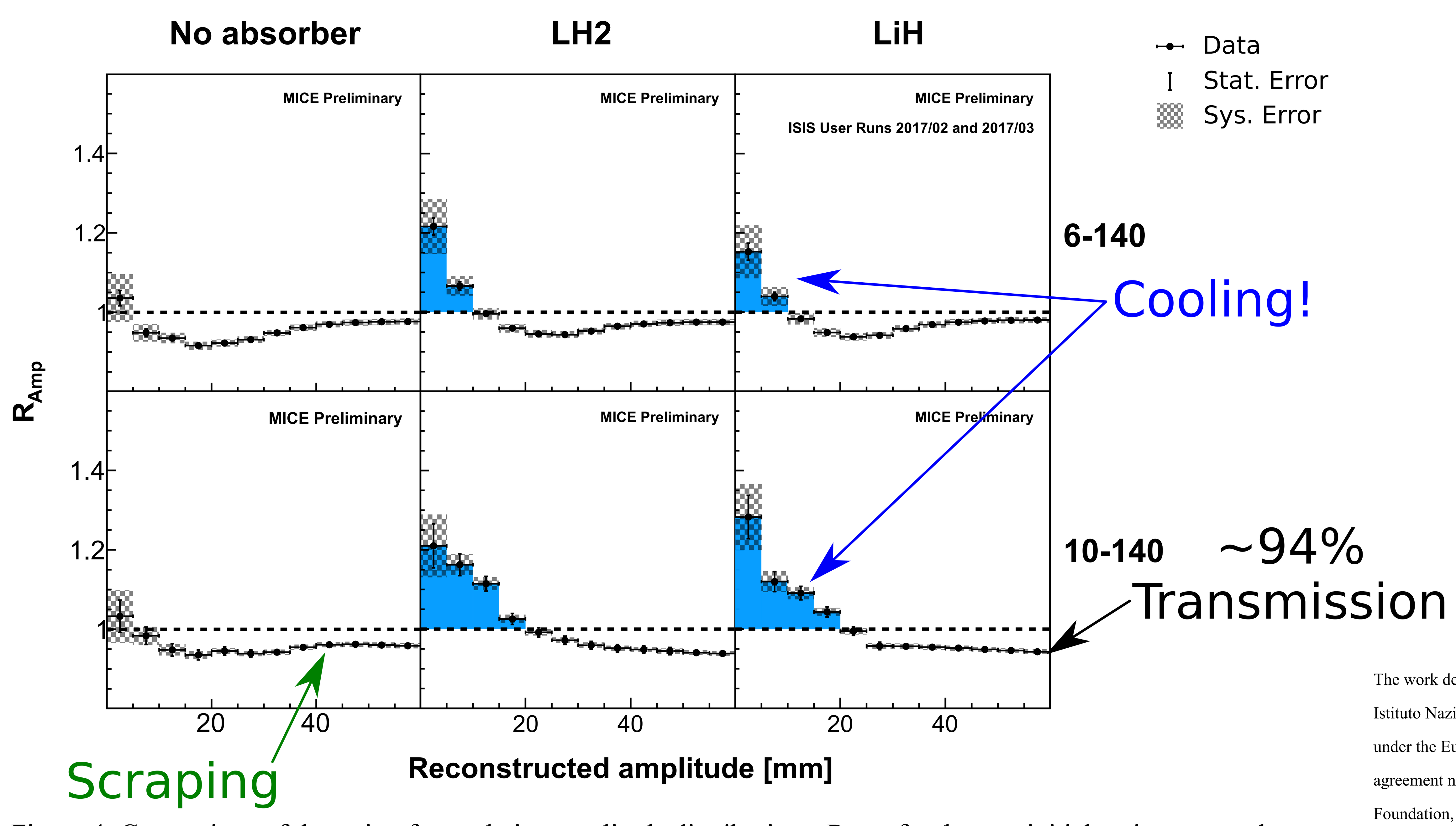

Figure 4: Comparison of the ratio of cumulative amplitude distributions, R_{Amp}, for the two initial emittances and three absorber configurations. Bins that deviate from a flat distribution demonstrate areas of migration.

ACKNOWLEDGEMENTS

The work described here was made possible by grants from Department of Energy and National Science Foundation (USA), the Istituto Nazionale di Fisica Nucleare (Italy), the Science and Technology Facilities Council (UK), the European Community under the European Commission Framework Programme 7 (AIDA project, grant agreement no. 262025, TIARA project, grant agreement no. 261905, and EuCARD), the Japan Society for the Promotion of Science and the Swiss National Science Foundation, in the framework of the SCOPES programme. We gratefully acknowledge all sources of support. We are grateful to the support given to us by the staff of the STFC Rutherford Appleton and Daresbury Laboratories and the Science and Technology Facilities Council. We acknowledge the use of Grid computing resources deployed and operated by GridPP in the UK, http://www.gridpp.ac.uk/.